

OPEN-LOOP, SELF-EXCITATION IN A BISTABLE MICROMECHANICAL BEAM ACTUATED BY A DC ELECTROSTATIC LOAD

L. Medina¹, R. Gilat², B. R. Ilic³, and S. Krylov¹

¹School of Mechanical Engineering, Faculty of Engineering, Tel-Aviv University, Ramat Aviv 69978, Israel

²Department of Civil Engineering, Faculty of Engineering, Ariel University, Ariel 44837, Israel

³Center for Nanoscale Science and Technology, National Institute of Standards and Technology, Gaithersburg, MD, 20899, USA

ABSTRACT

We demonstrate an open-loop self-excitation response in a curved, bistable microelectromechanical beam under a time-independent electrostatic load. The self-excitation is triggered by placing a high value resistor in series with a beam that is on the verge of bistability. The voltage-deflection curve of such a beam contains an inflection point, where the slope of the curve is approximately zero. Our results show that actuation at a voltage corresponding to the inflection point induces stable self-sustained oscillations. We further observe that implementation of the same actuation scenario in a bistable beam, with the voltage-deflection curve containing two stable branches, does not lead to self-excitation.

KEYWORDS

Curved micromechanical beam; Electrostatic actuation; Self-excitation; Bistability; MEMS/NEMS

INTRODUCTION

Self-excited systems are able to maintain stable oscillations under steady, time-independent, loading. Due to its beneficial features, this effect, which is also of fundamental scientific interest, has been employed in various applications, including atomic force microscopy [1,2], sensors [3,4] and energy harvesting [5].

In the realm of micro- and nanoelectromechanical systems (MEMS/NEMS), self-induced oscillations can be achieved using several approaches. The most common methods employ a closed-loop control, where an actuation voltage change, based on the velocity of the system, introduces nonlinear virtual damping [1,2,4]. Closed-loop control, proposed by S. S. Lee [6], includes an active amplification change of the driving electronic circuit for enhancing amplitude oscillations of the acoustic transducer. In general, closed-loop control at the micro- and nano-scale requires implementation of complex feedback algorithms [1,2,4] with demanding accuracy requirements for the position or velocity of the sensing transducer.

In contrast, open-loop devices take advantage of the structural intrinsic nonlinearities and interactions with their surroundings [3-8]. In these systems, self-induced oscillations are caused by parametric, configuration dependent forces. These forces result from nonlinear thermo-

opto-mechanical coupling [7] or electrostatically-induced structural contact with an actuating electrode [8,9]. Contact based systems may suffer from inferior reliability and long-term performance stability.

In this work, we report on experiments where self-sustained oscillations are triggered in an open-loop driven micromechanical device. We used an electrostatically-actuated, curved, bistable micromechanical beam. We show that self-excitation is an intrinsic property of such a beam, and can be achieved under appropriate conditions.

EXPERIMENT

Experimental Procedure & Equipment

Curved microelectromechanical beams (Fig. 1) were fabricated from a highly doped, single-crystal silicon device layer using a silicon-on-insulator wafer [10,11]. The structures were lithographically defined and etched using a deep reactive ion etching process. The structures were released by dissolution of the sacrificial oxide with hydrofluoric acid. After a high-pressure critical-point drying process, the device dimensions were measured using an environmental scanning electron microscope.

Micromechanical beams were designed with nominal dimensions of $b = 20 \mu\text{m}$, $d = 3.5 \mu\text{m}$, $g_0 = 10 \mu\text{m}$, $L = 1000 \mu\text{m}$ and nominal initial elevations of $h_0 = 0.5 \mu\text{m}$ and $h_0 = 2 \mu\text{m}$. Fabricated structural dimensions of the first beam were $d \approx 3.31 \mu\text{m}$, $g_0 \approx 10.97 \mu\text{m}$ and $h \approx 2.12 \mu\text{m}$. The second beam had a higher h with system dimensions of $d \approx 3.71 \mu\text{m}$, $g_0 \approx 10.37 \mu\text{m}$ and $h \approx 3.13 \mu\text{m}$. We attribute the discrepancy between the nominal and measured dimensions to the fabrication-related scatter in the geometric parameters due to residual stress, as discussed in our previous work [11,12].

Devices were mounted onto a wafer probing station and tested at room temperature under ambient air conditions. The electrical signal was generated and amplified by a factor of 20 using a signal processor and a high voltage amplifier, respectively. The in-plane motion of the beams was measured using an optical setup by video recording the beam's motion with a camera operating at a frame rate of $\approx 12 \text{ Hz}$. The beam midpoint position (w_m) corresponding to each video frame was determined using image processing technique [13].

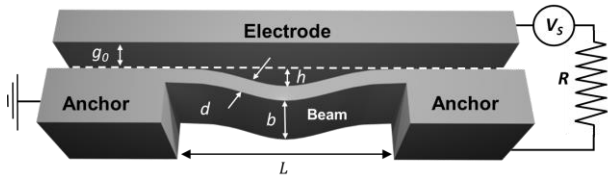


Figure 1: Schematics of a curved beam of length L , elevation h , thickness d , width b , beam to electrode distance g_0 , series resistor R and source voltage V_S .

Results & Discussion

Curved, micromechanical beams are characterized by their equilibrium curves, as Figure 2 illustrates. The plots were obtained using a reduced order (RO) model for a specified beam geometry [12]. Figure 2 presents two possible equilibrium curve scenarios for a curved beam used in our experiments. Figure 2(a) shows a beam on the verge of bistability with two limit, zero-slope, points labeled as the inflection and pull-in points. Figure 2(b) shows an equilibrium curve for a bistable beam characterized by three limit points: snap-through, release and pull-in points.

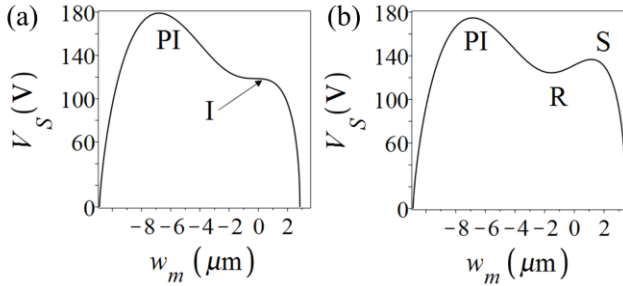


Figure 2: Reduced order model results: equilibrium curve for beams with $L = 1000 \mu\text{m}$, $b = 20 \mu\text{m}$, $d = 3.23 \mu\text{m}$, $g_0 = 10.88 \mu\text{m}$. (a) $h = 2.85 \mu\text{m}$ showing two limit points, a pull-in (PI) and an inflection point (I). (b) $h = 3.5 \mu\text{m}$ showing three limit points, snap-through (S), release (R) and pull-in (PI).

In our experiments, equilibrium curves were first obtained by applying a triangular voltage signal between the beam and the electrode. The maximum amplitude and duration of the signal were $\approx 30 \text{ V}$ and $\approx 60 \text{ s}$, respectively. A resistor $R \approx 10 \text{ k}\Omega$ was placed in series with the beam to limit current induced heating resulting from a possible pull-in collapse. Subsequently, static experiments with $R \approx 20 \text{ M}\Omega$ showed qualitatively similar beam motion with additional oscillations around the equilibrium curve. This procedure was carried out for two different beams. Figure 3 shows a response of a beam with $h \approx 2.12 \mu\text{m}$. The measured equilibrium curve shows that the beam is on the verge of bistability. This implies that instead of having a snap-through point, the beam has an inflection point [12]. The results presented in Fig. 4 superimposed against the applied triangular actuation signal, further show a gradual increase of vibrational amplitudes with increasing voltage. At the applied load of $\approx 20 \text{ V}$, vibrational amplitudes of $\approx 0.69 \mu\text{m}$ were observed.

Based on the results of the above experiment, we applied the following trapezoidal voltage signal

$$V_S(t) = V_{\max} \left(\frac{t}{T} (1 - H(t - T)) - \frac{t - 2T}{T} H(t - 2T) \right) \quad (1)$$

where t is time, $H(t)$ is the Heaviside step function. The maximum voltage signal was $V_{\max} \approx 20 \text{ V}$, with time $T \approx 30 \text{ s}$ for each of the three trapezoidal segments: linearly increasing ramp, constant and a linearly decreasing ramp. Figure 5 shows the beam response to the trapezoidal signal.

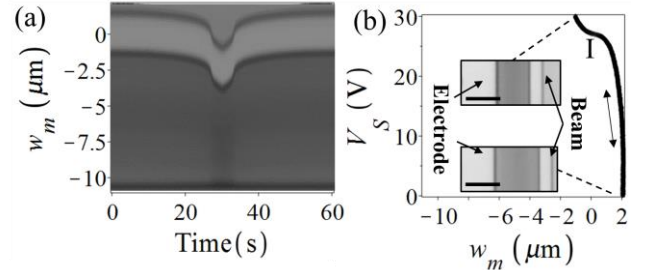


Figure 3: Experimental results: a quasi-static experiment with $R \approx 10 \text{ k}\Omega$, $L \approx 1000 \mu\text{m}$, $b \approx 20 \mu\text{m}$, $d \approx 3.32 \mu\text{m}$, $h \approx 2.12 \mu\text{m}$, and $g_0 \approx 10.97 \mu\text{m}$. (a) Direct visualization of the time history. (b) Static buckling curve. Insets represent snapshots of the initial position and maximum deflection corresponding to the highest voltage $V_{\max} \approx 30 \text{ V}$. Scale bars represent $\approx 10 \mu\text{m}$. The two-directional arrows represent the beam midpoint movement along the equilibrium curve. Label I denotes the inflection point.

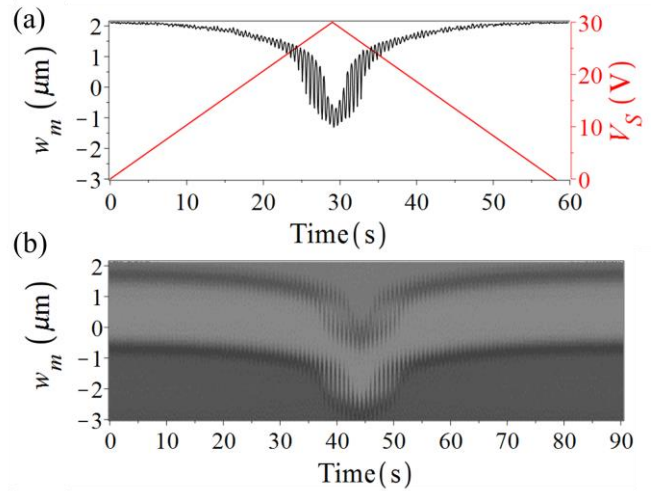


Figure 4: Experimental time history results for the beam with dimensions defined in Figure 3 with $R \approx 20 \text{ M}\Omega$: (a) Time history of the beam midpoint motion (black) and the source voltage (red). (b) Direct visualization of the time history.

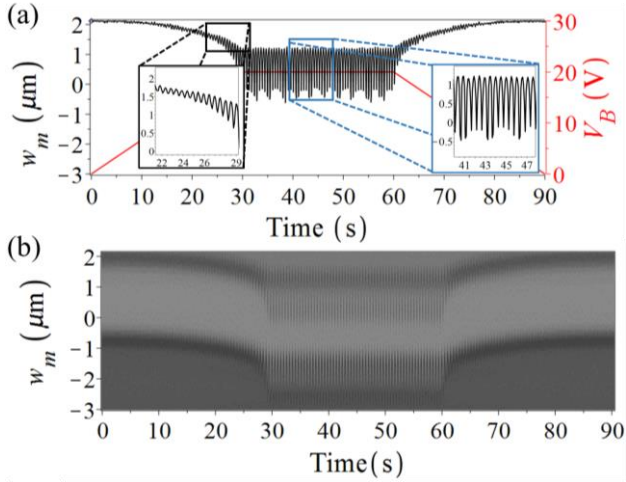


Figure 5: Experimental results of the beam from Fig. 3 with $R \approx 20 \text{ M}\Omega$. The voltage signal consisted a linearly increasing ramp, a constant region with $V_{max} \approx 20 \text{ V}$, and a decreasing ramp (red curve): (a) Time history. The black and blue framed insets represent zoomed-in figure data. (b) Direct visualization of the time history.

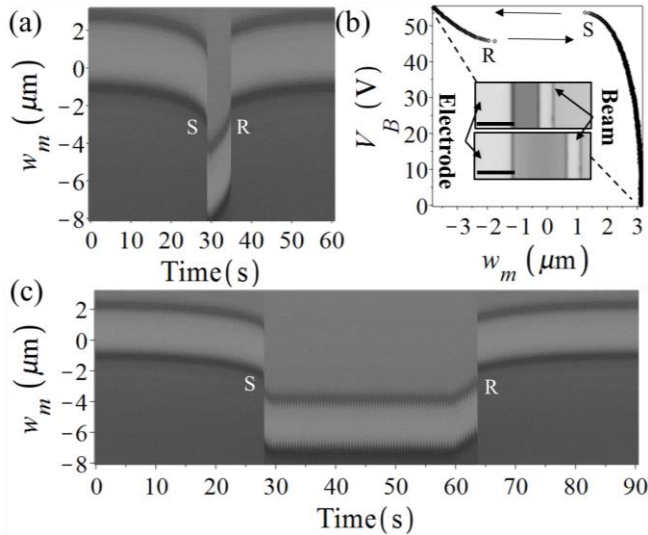


Figure 6: Results of experiments on a bistable beam with $L \approx 1000 \mu\text{m}$, $b \approx 20 \mu\text{m}$, $d \approx 3.71 \mu\text{m}$, $h \approx 3.14 \mu\text{m}$, $g_0 \approx 10.37 \mu\text{m}$. (a) Direct visualization of the time history and (b) buckling curve with snapshots of the beam with $R \approx 10 \text{ k}\Omega$ under a triangular signal. Insets represent the initial position and maximum deflection corresponding to the highest voltage $V_{max} \approx 55 \text{ V}$. Scale bars represent $\approx 10 \mu\text{m}$. The arrows represent the beam midpoint direction upon loading-unloading triangular signal. (c) Direct visualization of the response of the beam with $R \approx 20 \text{ M}\Omega$ to a trapezoidal voltage signal of amplitude $V_{max} \approx 50 \text{ V}$, and total duration of $3T \approx 90 \text{ s}$. S and R represent snap-through and release points.

We observed high amplitude oscillations in the region of constant bias ($\approx 30 \text{ s} < t < \approx 60 \text{ s}$). Figure 5 insets show the measured beam response during the linearly

increasing voltage ramp (black frame inset) and in the region with $V_{max} \approx 20 \text{ V}$ (blue frame inset). With the frame rate of $\approx 12 \text{ Hz}$, even though the full time history of the oscillatory behavior is not fully apparent, the boundaries of the response are visible, yielding a maximum oscillatory amplitude of $\approx 1.66 \mu\text{m}$.

To gain further insight into the conditions for the observed self-excitation, the behavior of a bistable [10] curved beam with $h \approx 3.13 \mu\text{m}$ under a triangular signal with $T \approx 60 \text{ s}$ was examined and is shown in Fig. 6. For the case of $R \approx 10 \text{ k}\Omega$, the quasi-static response and the corresponding equilibrium curve, Fig. 6(a) and (b) show bistability with a clear distinction between the snap-through and release limit points. Figure 6(c) shows that a trapezoidal signal with $V_{max} \approx 50 \text{ V}$ and $R \approx 20 \text{ M}\Omega$ did not produce large amplitude self-excited oscillations. The observed oscillations had a maximum amplitude of $\approx 0.16 \mu\text{m}$, which is smaller than the distance between the two stable equilibria of the bistable beam. These results imply that in order to induce self-oscillations, the difference between the snap-through and the release voltages should be small. This condition is satisfied when the beam is on the verge of bistability, where the snap and release points coincide.

SUMMARY & CONCLUSIONS

Our work demonstrates a first instance of self-oscillatory behavior of curved, bistable, micromechanical beams electrostatically actuated by a single electrode in an open-loop configuration. We experimentally showed that self-induced oscillations occur when an additional, sufficiently large, resistance is added in series with the microelectromechanical beam. Our observations suggest that the development of high amplitude vibrations is possible when the curved beam is on the verge of bistability. This requirement allows vibrational shifting along the zero slope part of the equilibrium curve around an inflection point.

The self-excitation is attributed to the influence of a large resistor which limits the charging current and therefore increases the capacitor charging time. As the beam moves quasi-statically, wherein the rate of motion is much slower than the capacitor charging rate, the beam is in equilibrium at any point. Alternatively, when the beam approaches and passes the inflection point, where the slope of the voltage-displacement curve is close to zero, the rate of motion increases. Since the electric current, limited by the resistor, is not sufficient to charge the capacitor, the effective electrode voltage drops. As a result, the beam is in a non-equilibrium state, where the elastic restoring force is larger than the electrostatic force. This configuration corresponds to smaller beam deflections and decreased capacitance. The consequent voltage increase sets the beam to a non-equilibrium configuration, where the actuating electrostatic force is higher than the restoring mechanical force. This process repeats, thereby producing self-sustained vibrations.

ACKNOWLEDGEMENTS

The devices were fabricated and tested at the Center for Nanoscale Science and Technology (CNST) at the National Institute of Standards and Technology and at the Tel Aviv University MEMS design and characterization lab (MDCL). The authors would like to thank Stella Lulinski in helping with the presented work. The research is supported by the Israel Science Foundation (ISF grant no. 1272/16), Israel Ministry of Science, Technology and Space and Ariel University.

REFERENCES

- [1] Yabuno, H., Kaneko, H., Kuroda, M., & Kobayashi, T. (2008). Van der Pol type self-excited micro-cantilever probe of atomic force microscopy. *Nonlinear Dynamics*, 54(1-2), 137-149.
- [2] Lee, C., Itoh, T., & Suga, T. (1999). Self-excited piezoelectric PZT microcantilevers for dynamic SFM— with inherent sensing and actuating capabilities. *Sensors and Actuators A: Physical*, 72(2), 179-188.
- [3] Sung, S., Lee, J. G., Lee, B., & Kang, T. (2003). Design and performance test of an oscillation loop for a MEMS resonant accelerometer. *Journal of Micromechanics and Microengineering*, 13(2), 246.
- [4] Lee, Y., Lim, G., & Moon, W. (2006). A self-excited micro cantilever biosensor actuated by PZT using the mass micro balancing technique. *Sensors and Actuators A: Physical*, 130, 105-110.
- [5] Wang, Z., Li, Z., & Lu, W. (2007, October). A new self-oscillation loop for MEMS vibratory gyroscopes. In 2007 7th International Conference on ASIC.
- [6] Lee, S. S., & White, R. M. (1996). Self-excited piezoelectric cantilever oscillators. *Sensors and Actuators A: Physical*, 52(1), 41-45.
- [7] Aubin, K., Zalalutdinov, M., Alan, T., Reichenbach, R. B., Rand, R., Zehnder, A., Parpia, J. & Craighead, H. (2004). Limit cycle oscillations in CW laser-driven NEMS. *Journal of Microelectromechanical Systems*, 13(6), 1018-1026.
- [8] Bienstman, J., Vandewalle, J., & Puers, R. (1998). The autonomous impact resonator: a new operating principle for a silicon resonant strain gauge. *Sensors and Actuators A: Physical*, 66(1), 40-49.
- [9] Shmulevich, S., Hotzen, I., & Elata, D. (2015, January). The electromechanical response of a self-excited MEMS Franklin oscillator. In *IEEE MEMS 2015 28th International Conference* (pp. 41-44). IEEE.
- [10] Krylov, S., & Dick, N. (2010). Dynamic stability of electrostatically actuated initially curved shallow micro beams. *Continuum Mechanics and Thermodynamics*, 22(6-8), 445-468.
- [11] Krylov, S., Ilic, B. R., Schreiber, D., Seretensky, S., & Craighead, H. (2008). The pull-in behavior of electrostatically actuated bistable microstructures. *Journal of Micromechanics and Microengineering*, 18(5), 055026.
- [12] Medina, L., Gilat, R., & Krylov, S. (2014). Symmetry breaking in an initially curved pre-stressed micro beam loaded by a distributed electrostatic force. *International Journal of Solids and Structures*, 51(11), 2047-2061.
- [13] Medina, L., Gilat, R., Ilic, B., & Krylov, S. (2014). Experimental investigation of the snap-through buckling of electrostatically actuated initially curved pre-stressed micro beams. *Sensors and Actuators A: Physical*, 220, 323-332.

CONTACT

*L. Medina; liormedi@post.tau.ac.il